Long-term stability of a backfilled room-and-pillar test section at the Buick Mine, Missouri, USA

D.R. Tesarik [a,*], J.B. Seymour [a], T.R. Yanske [b]

[a] NIOSH-Spokane Research Laboratory, 315 E. Montgomery Avenue, Spokane, WA 99207
[b] The Doe Run Company, Buick Mine/Mill, HC1 Box 1390, Highway KK, Boss, MO 65440

A B S T R A C T

Rock mechanics instruments have been providing data in a backfilled room-and-pillar test section of the Buick Mine near Boss, Missouri, USA, for nearly 16 years. Host rock instruments include borehole extensometers installed in the mine roof and pillars, and biaxial stressmeters used in pillars and abutments. Embedment strain gauges, extensometers, and earth pressure cells were installed in the cemented backfill. The instruments monitored stability of the test section for two years while the pillars were extracted, and 14 years after pillar extraction to monitor long-term stability. Of the transducers that were not mined out when the pillars were extracted, 68% still function. Data from these instruments demonstrate that backfill improves long-term underground safety by supporting the mine roof and maintaining the strength of support pillars. For example, backfill significantly limited the dilation of a remaining support pillar by providing confinement on one side of the pillar. Post-mining stress and strain in the backfill account for 35% and 28% of the total stress and strain that was measured, respectively. Earth pressure cell stress measurements confirmed visual observations that the backfill remained stable. Post-mining stress measurements from the earth pressure cells fit natural log equations as a function of time with *r*-squared values ranging from 0.76 to 0.98. Natural log equations also described post-mining strain behavior of the backfill with *r*-squared values ranging from 0.30 to 0.99. Stresses calculated for the backfill by a three-dimensional numerical model of the test area were consistent with those that were measured by earth pressure cells.

1. Introduction

Several important factors affect the stability of underground excavations including in situ stress, rock mass properties, opening spans, and time since excavation [1]. With the loss of confining forces on the rock mass after mining, ground conditions are subject to deterioration, such as pillar spalling, caving of the mine roof, and roof-to-floor or wall-to-wall convergence. This process continues with time and threatens long-term stability. Backfill is placed in underground openings prior to pillar extraction to slow down this time-dependent failure by providing confinement and support for the rock mass, thereby limiting the amount of convergence. In many cases, long-term mining would be impossible without the use of backfill because it also provides regional stability [2,3].

Backfill can also be subject to long-term loading as stresses are gradually transferred from the host rock with time. Compaction, settlement, and movement of backfill from this additional load can affect regional mine stability. Long-term regional stability of the backfill is essential when an access way must remain open adjacent to a backfill-supported area or when there are active mine workings near the backfilled section. Geotechnical instruments provide an important means of monitoring and quantitatively evaluating the stability of backfilled mine sections so that appropriate actions can be taken to address stability concerns [4].

The duration of a rock mechanics instrumentation project is determined in part, by the goals of the project, long-term accessibility of the instrument cables, and susceptibility of instruments and their cables to damage from mining activity. The following citations are examples of backfill-related monitoring programs lasting less than six years. McNay and Corson [5] measured wall closure and stress in a cut-and-fill vein mine for over five years to quantify the effectiveness of hydraulic sandfill on wall closure. Hergot and Munroe [6] monitored backfill stresses and roof deformation in a potash mine for nearly two years to assess the time required for waste salt placed as backfill to provide roof support. Beddoes et al. [7] monitored backfill stresses in mill tailings and wall deformations in a cut-and-fill stoping system for approximately one year at a potash mine to determine the consolidation and strength development of mill tailings and the effect of backfill on wall closure. A monitoring program was performed by Gürtunca et al. [8] for nearly two years

*Corresponding author. Tel.: +1 509 354 8052; fax: +1 509 354 8099.
E-mail address: det4@cdc.gov (D.R. Tesarik).

to quantify the performance of cemented tailings on hanging wall closure and compare the results to the performance of timber-pack support systems. Pore-pressure was measured for approximately two years by Zhurin [9] in tailings deposited in an underground iron ore deposit to estimate drainage time and determine interaction between stopes. Donovan et al. [10] instrumented three sill mat sections with multiple-point borehole extensometers to measure vertical displacement of overlying paste fill when it was undercut, earth pressure cells to measure horizontal pressure, and contractometers along with extensometers to measure wall closure for about one year.

Rock mechanics programs with the primary objective to evaluate long-term behavior of host rock and backfill necessarily require a longer data collection period. De Sousa et al. [4] monitored a grout and backfill system to control brine inflow and monitor long-term stability for 10 years. Maleki et al. [11] analyzed nine years of convergence measurements collected at a proposed site for an underground repository for the permanent disposal of radioactive waste to determine long-term stability of a section of the repository.

Backfill was first tested at the Buick Mine in an instrumented test section to determine if the support pillars that remained after primary extraction could be mined safely and economically. Quantifying the residual strength of failed pillars surrounded by backfill, or "trapped" pillars, was of particular interest because of their potential to stabilize the mine roof and reduce loads on surrounding pillars [12]. The instruments that remained after mining the pillars in the test section were read for an additional 14 years to monitor long-term stability and quantify time dependent behavior in the mine roof and backfill.

1.1. Buick Mine

As shown in Fig. 1, the Buick Mine is one of six underground mines in the New Lead Belt, or Viburnum Trend, that is owned and operated by the Doe Run Company, St. Louis, Missouri. The New Lead Belt is a flat-lying, tabular ore deposit containing lead, zinc, and copper that lies under 150–360 m of overburden. The ore body is 1–40 m thick, 10–600 m wide, and has a trend length of 65 km. Fig. 2 illustrates the rock types using a generalized stratigraphic column. The mining horizon consists of competent

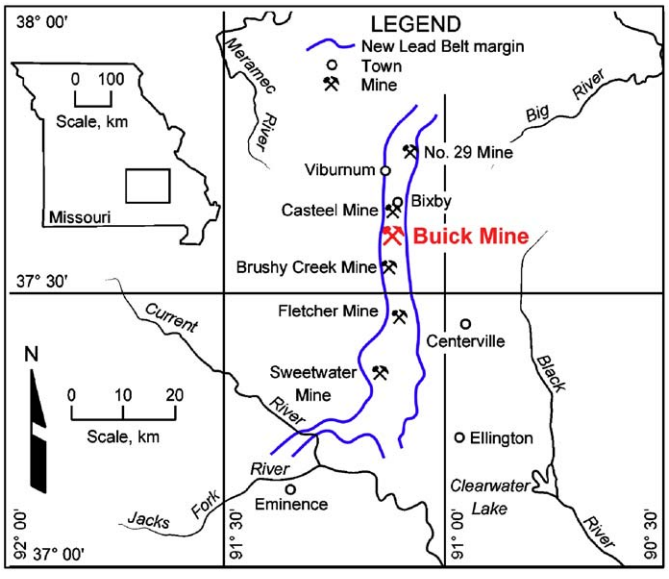

Fig. 1. Operating mines in the New Lead Belt (Viburnum Trend), Missouri, USA.

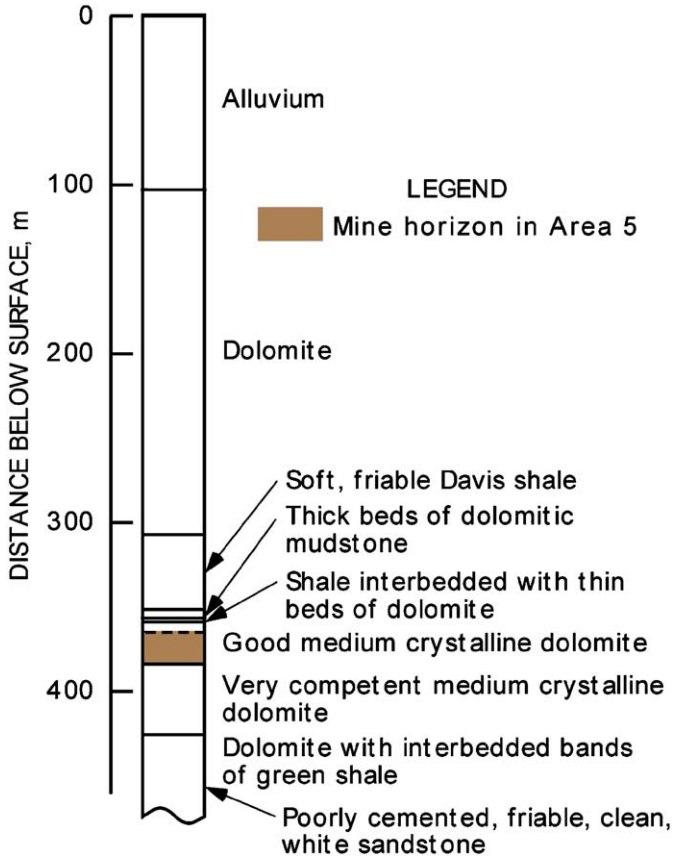

Fig. 2. Generalized stratigraphic column of Area 5.

dolomite with a roof composed of interbedded dolomite, shale, and dolomitic mudstone. A 43-m-thick layer of Davis shale lies above these beds followed by competent dolomite to the weathered surface. The deposit has two main joint sets and one set of horizontal bedding planes with discontinuities spaced from 13 cm to 2 m. One joint set trends N45°E and dips 70–90° to the southeast, and the other trends N45°W and dips 70–90° to the southwest. The dolomitic host rock has an average unconfined compressive strength (UCS) of 108.9 MPa and a rock mass rating (RMR) of 72 [13].

Mining equipment used for primary room development at the Buick Mine includes two-boom drill jumbos, 7- to 9-ton-capacity loaders, and 27- to 45-ton-capacity haul trucks. Secondary mining includes back, bottom, undercut, and overcut passes. In sections to be backfilled, either 1.8- to 2.4-m-long split sets or 1.8- to 2.4-m-long resin-grouted rebar bolts are installed, depending on ground conditions [14].

Cemented rockfill (CRF) is used during pillar extraction to provide area stability. To contain the CRF, uncemented 1.8-m-high waste rock berms are first constructed between pillars around the perimeter of the area to be backfilled. Several CRF lifts are then placed between the berms to a height of 1.8 m. Fill fences consisting of 13-mm steel cables and #4-gauge welded wire panels are constructed from this CRF platform. The steel cables are looped through angle brackets secured to the pillar ribs with expansion anchor bolts. If the fence height exceeds 9 m, two evenly spaced tieback anchors are placed in the fill to support each support cable of the steel fence. Additional 1-m lifts are placed to within 1 m of the top of the fill fence. This construction procedure is repeated until the CRF is 0.6 m from the mine roof if a slinger truck is used to fill the final gap. In this case, the top-off

material is a mixture of minus 5-cm waste rock, cement, fly ash, water, and cycloned mill tailings. If a grout pump is used, the final gap is 15 cm and filled with a mixture of mill tailings, water, cement, fly ash, foaming agent, and a retarder [15,16]. After the area is backfilled, ore pillars on the perimeter of the backfilled section are mined, and trapped pillars are either left for support or mined from a sublevel drift.

1.2. Backfill test section

A section called Area 5, shown in plan view in Fig. 3, was the first place that backfill was used at the Buick Mine. Area 5 was chosen because this section of the mine was surrounded by barrier pillars that could arrest redistributed loads of a cascading pillar run if it occurred during the test. These pillars were approximately 8–12 m wide per side and 18 m high. The entire backfilled area measured 88 m x 37 m. Rooms were approximately 9.8 m wide. Fig. 4 is a photograph of the south side of the test section.

The test area was backfilled with CRF that was produced by combining minus 1-m run-of-mine waste rock with waste rock that had been crushed to minus 13 cm and mixed at an underground batch plant with cycloned mill tailings and about 4% cement [17]. The dolomite waste rock that was used for CRF aggregate was quarried underground [18]. The CRF was

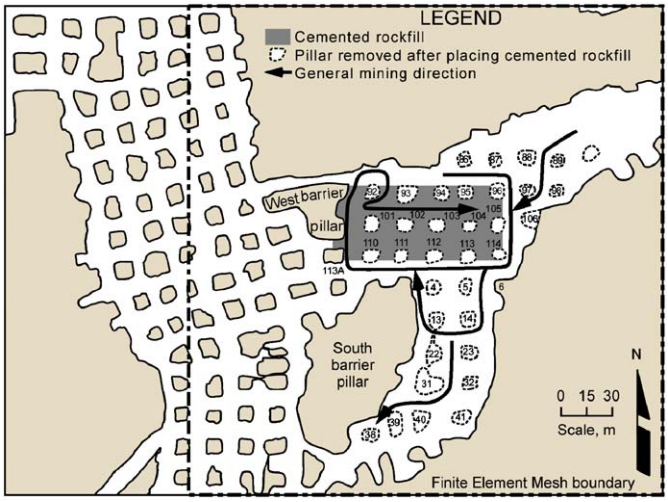

Fig. 3. Plan view of Area 5.

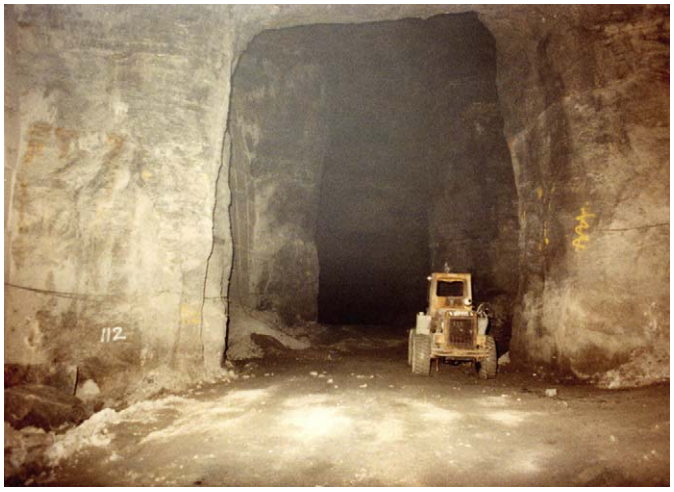

Fig. 4. Pillars in Area 5.

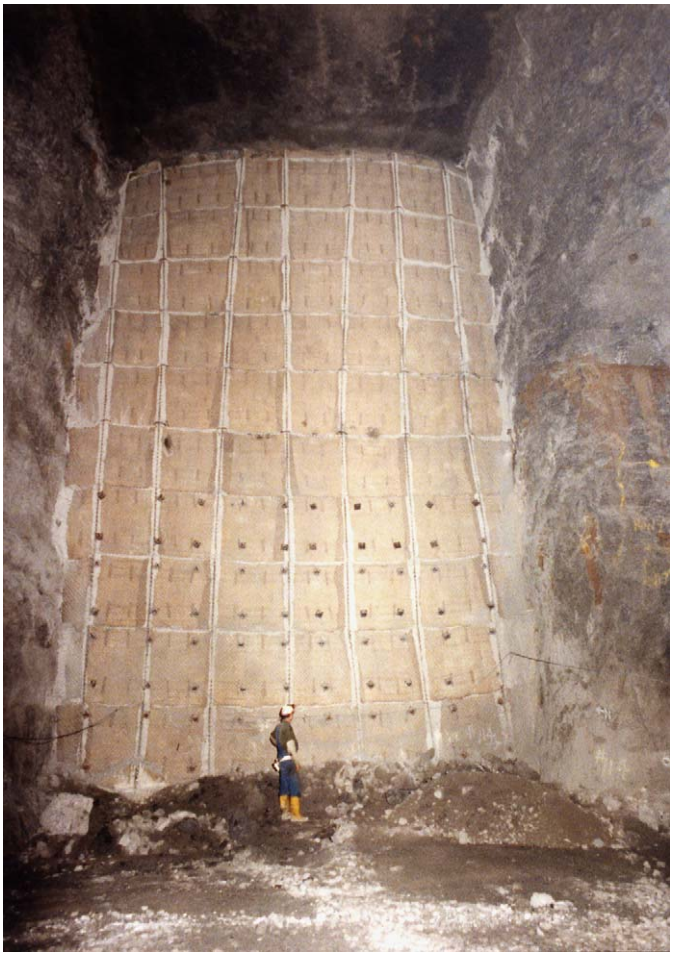

Fig. 5. Steel-reinforced shotcrete fill fence.

transported to the backfill section by conveyor and spread in 0.3- to 0.6-m lifts using wheeled dozers. The CRF was placed in contact with the pillar ribs and the rib of the west barrier pillar. As lifts of backfill were placed, a steel-reinforced shotcrete fence was constructed sequentially from the floor to the mine roof between the perimeter pillars to contain the CRF. One of the completed fill fences is shown in Fig. 5. In addition, square shotcreted cyclone fences with 1.5-m sides were constructed sequentially from floor to roof on the north sides of the four trapped pillars which were confined by CRF on all four sides. The inside of these enclosures were left empty to serve as free faces when the pillars were blasted. The top 3 m of backfill had a maximum aggregate diameter of 5 cm and was placed with front-end loaders and slinger trucks [15]. From visual inspections, approximately 50% of the backfill was in contact with the mine roof, and the maximum gap between the top of the backfill and remaining area was about 1 cm.

Table 1 contains the mining sequence and it is shown graphically in Fig. 3. In general, the pillars in the drift northeast of the backfilled section were mined first, followed by the pillars along the perimeter of the backfill, and then pillars 101–104 which were surrounded by backfill. The trapped pillars were drilled and blasted from an access drift approximately 6 m below the test area. About 3.5 years after the last trapped pillar was mined, eight additional pillars were mined south of this area between the south barrier pillar and east abutment [19].

Since 1991, 12.7 million tons of pillar ore have been mined at Doe Run's mines in the New Lead Belt, using 5.4 million tons of CRF. Pillar extraction currently accounts for 26% of rock mined annually. However, because of their high grade, the mined pillars

Table 1
Pillar extraction sequence, elapsed time in days.

Pillar	Day
97, East half	0
96	17
87, South half	17
97, West half	17
95	52
86, South half	52
94	59
105	85
106	85
114	101
5, North half	123
113, Bottom 12.5 m	123
6, West 3.7 m	123
113, Top 4.3 m	127
5, South half	177
14, North half	177
112	192
4, North half	192
4, South half	199
13, North half	199
111	212
110	212
93	221
92	233
101	389
102, 7 Holes	444
102, 20 Holes	451
104	515
103	695
23	1974
22	1984
32	2000
31	2010
41	2048
40	2109
38	2179
39	2181

currently account for 38% of the lead, 34% of the zinc, and 24% of the copper metal that is produced annually. Doe Run has 17.2 million tons of pillar reserves.

2. Instrumentation

Borehole extensometers and biaxial stressmeters were installed in the pillars and abutments of Area 5. Extensometers were also installed in the mine roof. Embedment strain gauges and earth pressure cells were placed at mid-height and near the top of the cemented backfill as shown in Fig. 6. Full convergence measurements were not taken because these instruments and their cables could not be properly protected from mining equipment and blast damage during backfilling or pillar removal. The purpose of the instruments was to monitor short- and long-term stability, record stress redistribution to pillars during mining, provide input to calibrate a numerical model, and calculate rock mass modulus and strength. Measures taken to ensure that components of the measurement system would cause minimal error are discussed below.

2.1. Transducers

All of the instruments used in this study, except for the backfill extensometers, were manufactured by Geokon, Inc.[1] Vibrating

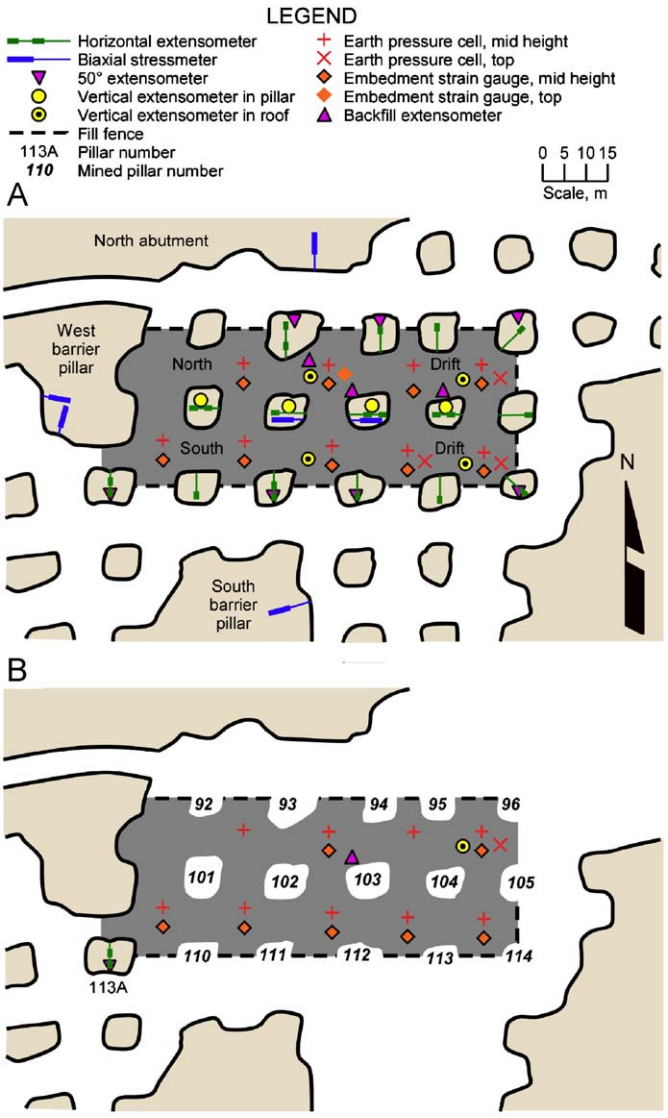

Fig. 6. Instruments in Area 5. A: Instruments originally installed; B: instruments functioning 16 years after installation.

wire transducers were used in all of the instruments because of their proven longevity, stability, and minimal zero drift over long time periods [20–22]. Another important feature of vibrating wire instruments is that their readings are not affected by a change in resistance of the lead wires. This eliminates the need to retrieve and recalibrate the instrument if broken wires are spliced. None of the instruments that were installed in this study were retrieved because they were either covered with backfill, grouted in boreholes, or located in inaccessible areas after pillar mining was completed.

Geokon, Inc. is conducting an on-going long-term test with eight 4500-series pressure transducers set at different initial frequencies to determine if zero drift develops with time. The operating principle of these pressure transducers is similar to that of the earth pressure cells that were used in Area 5. Each transducer is equipped with a vibrating wire element attached to a pressure sensitive diaphragm. As fluid pressure acting on the diaphragm changes, it causes the diaphragm to deflect, which in turn produces a change in tension and thus a change in the frequency of the vibrating wire [23]. Results from Geokon's laboratory test, presented in Fig. 7, indicate that all of the

[1] Mention of any company or product does not constitute endorsement by the National Institute for Occupational Safety and Health.

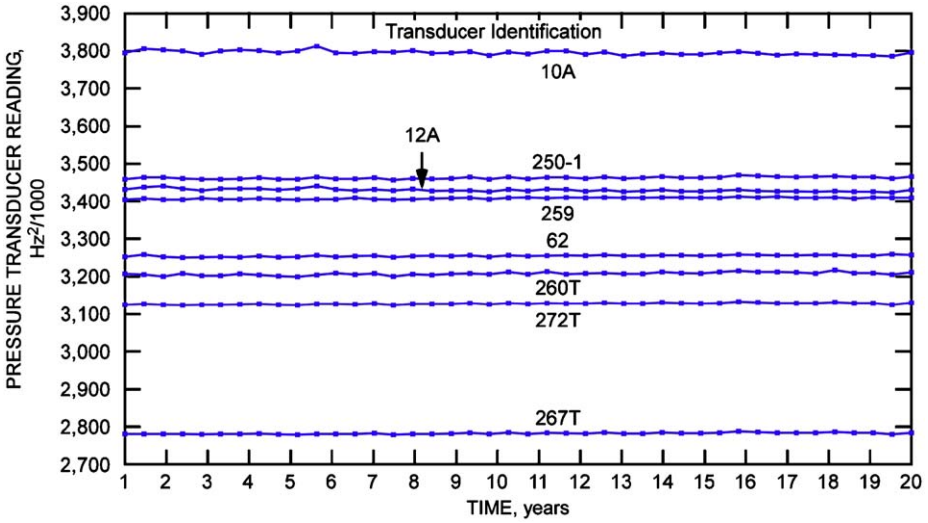

Fig. 7. Long-term stability data for Geokon, model 4500 series, pressure transducers (courtesy of Geokon, Inc.).

transducers have insignificant drift and repeatable readings over a period of 20 years.

Laboratory tests with vibrating wire displacement transducers also demonstrate that these transducers provide reliable long-term readings. The displacement transducer consists of a vibrating wire that is connected in series with a spring and a connecting rod. Movement of the rod changes the tension in the spring and consequently produces a corresponding change in the tension and the resonant frequency of the vibrating wire. A displacement transducer tensioned to 50% of full scale for 1,215 days exhibited no significant zero drift, and repeatability was well within $\pm 0.5\%$ full scale of the gauge [20]. These tests along with those conducted by Geokon, Inc. indicate that instrument measurements in Area 5 are a function of material behavior and not instrument error.

2.2. Cables

To protect the transducer signal from electrical noise, each pair of lead wires in the instrument cable is wrapped in Mylar tape with an aluminum foil shield. A bare copper wire is routed with each pair of lead wires to drain any induced currents to ground. An additional drain wire is added to the bundle of pairs and wrapped with another layer of Mylar tape [21]. Direct-burial cables with thick polyurethane jackets are used to protect the encased wires from sharp edges of the aggregate used in the backfill. For additional protection, the instrument cables were placed in slotted steel pipes and covered with ventilation fabric. About 0.5 m of backfill was placed over the pipes, earth pressure cells, and embedment strain gauges and allowed to cure for at least one day before heavy machinery was driven over them.

2.3. Dataloggers

Three Campbell Scientific, Inc. dataloggers were used to synchronize the instrument readings. A shed was placed near the west barrier pillar to protect the dataloggers from blast fly rock and mining equipment. Data collection began after backfilling was completed and all the instrument cables were connected to the dataloggers, which was 101 days after the first instruments were installed. Instrument readings were automatically recorded every 2 h except before and after some pillar blasts; for these cases, the interval was shortened to 10 min to capture immediate pillar response to the blast. Manual readings for instruments that were not mined out or damaged during pillar mining were recorded every one to two years, for the next 14 years.

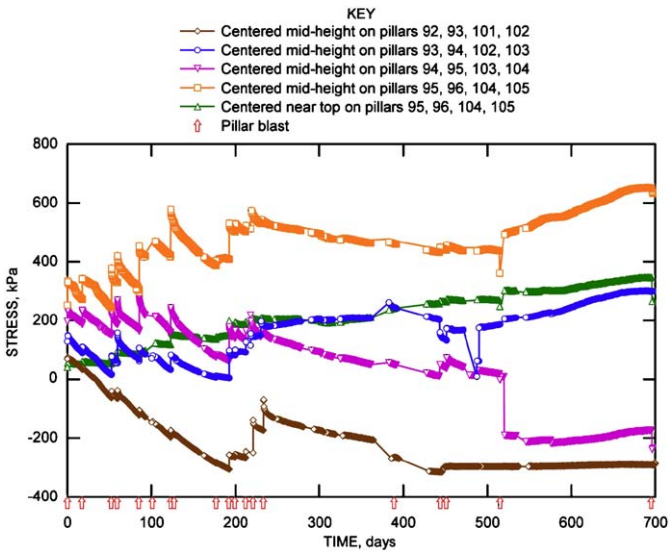

Fig. 8. Stress versus time for earth pressure cells in north drift.

2.4. Temperature effect

Laboratory tests [24], field investigations [25], and theoretical calculations [26] indicate that temperature change can significantly affect the magnitude of stress that is recorded by an earth pressure cell. For example, a temperature rise of 34 °C resulted in a temperature-induced stress increase in an earth pressure cell equal to 830 kPa when the earth pressure cell was covered with a thin layer of shotcrete [25]. Correction factors are available from manufacturers but these factors account for a small percentage of the temperature effect on the instrument because they compensate only for the transducer and not the entire instrument body [25].

In this study, cooling of CRF is characterized by apparent decreases in the stress or strain measured in the backfill between

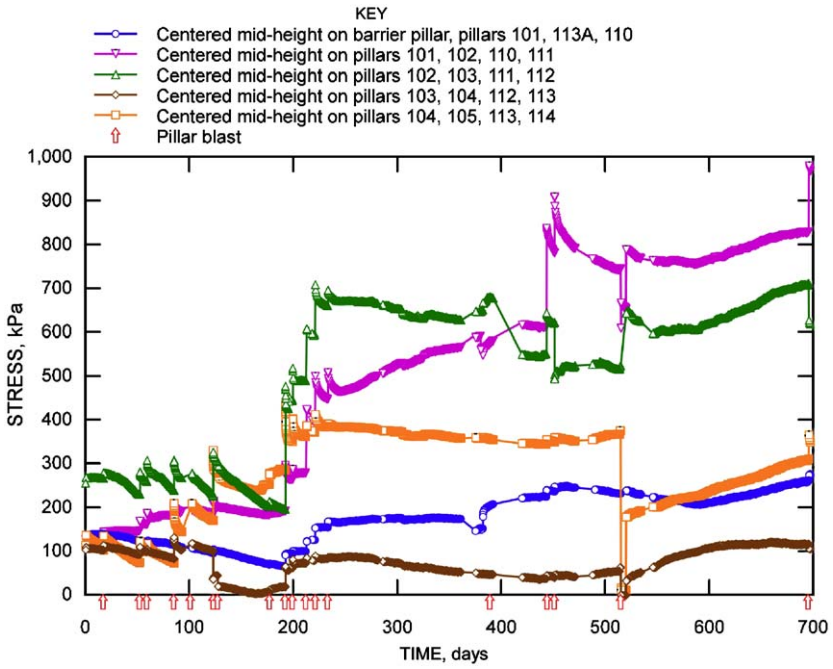

Fig. 9. Stress versus time for earth pressure cells in south drift.

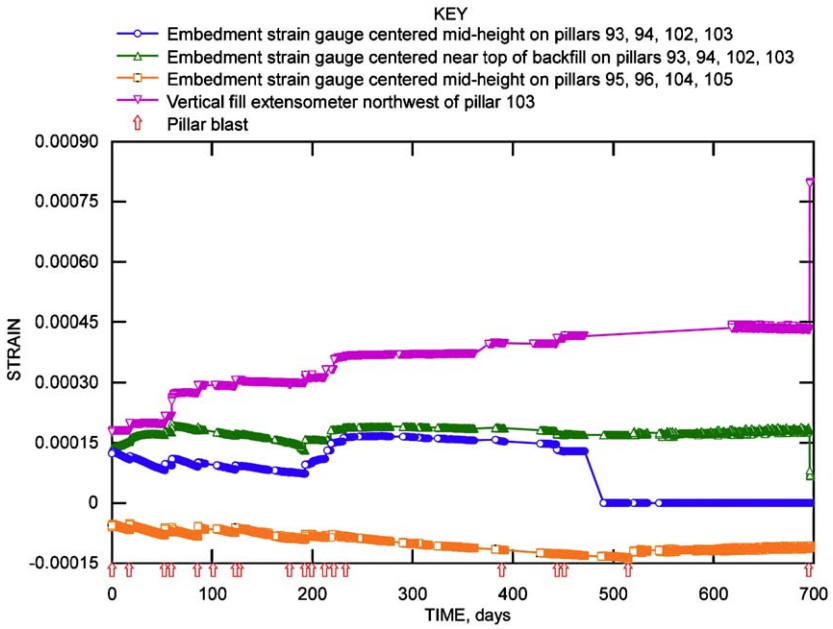

Fig. 10. Strain versus time for embedment strain gauges and vertical fill extensometer in north drift.

blasts as shown in Figs. 8–11. Based on previous field, laboratory, and theoretical studies, these decreases are assumed to be primarily temperature induced and were not included in calculations of total stress or strain change measured in the backfill. The total stress or strain change in the backfilled area caused by pillar mining was calculated by summing the change caused by the weight of backfill placed over the instruments, the change that was recorded immediately after each pillar was mined, the positive time-dependent change between blasts, and the abrupt changes not associated with a mining event. This sum does not account for time-dependent loading from the mine roof that was masked by temperature-induced decreases in readings. Consequently, reported values may be smaller than the actual stress or strain that occurred in the backfill during mining.

Readings recorded by the borehole extensometer installed in the mine roof centered on pillars 95, 96, 104, and 105 indirectly show that temperature did not change significantly between days 451 and 515. Strain is plotted as a function of time for this borehole extensometer in Fig. 12. Because strain caused by tensile displacement in the mine roof and strain induced by CRF cooling are both in the positive direction for this instrument, small changes in readings between blasts indicate that the tensile strain in the mine roof has stabilized by day 451 and imply that the temperature change in the immediate roof is negligible.

3. Instrument placement

When the CRF was mid-height to the pillars, it provided a working platform for installing horizontal extensometers and biaxial stressmeters in the support pillars and placing earth pressure cells and embedment strain gauges in the north and south drifts at the mid-height level of the backfill.

3.1. Backfill instruments

Model 4800E earth pressure cells were used to measure vertical stress change in the backfill. These 23-cm-diam instruments have a maximum load capacity of 6.9 MPa [23]. Before the earth pressure cells were placed in the CRF, they were cast in wood forms with minus 0.64-cm cemented aggregate and cured for several weeks. The forms were removed before they were placed in the backfilled drifts.

The model VCE-4210 embedment strain gauges were 25.4 cm long with 5-cm-diam steel flanges at each end. A steel wire-and-spring assembly is tensioned between the flanges in 2.54-cm-diam tubing and custom-built to provide up to 0.64 cm of relative displacement, or about 25,000 με [23]. They were cast in nominal 15-cm-diam x 30-cm-long cardboard cylinders with the same material as the earth pressure cells. Casting the instruments prior to their installation in the backfilled drifts helps protect them from the large aggregate in the CRF and also helps maintain their alignment when they are covered with wet backfill.

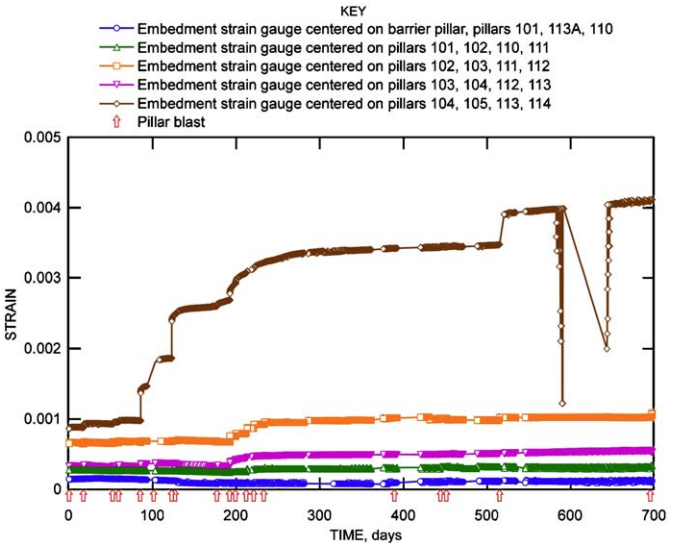

Fig. 11. Strain versus time for embedment strain gauges located mid-height to pillars in south drift.

To measure relative vertical backfill displacement over a large distance, three 4.2-, 11.0-, and 16.5-m-long vertical extensometers were assembled as the backfill was placed [18]. A 46-cm-square steel plate was used as the bottom bearing surface of the instrument to which a 5.1-cm-diam pipe coupler was welded. A section of steel pipe was threaded into the coupler, and additional sections were added as the height of the backfill increased. Sections of steel rod were coupled inside the steel pipe to connect the bottom plate to the vibrating wire transducer and top bearing plate. A steel cover was bolted to the top plate to protect the transducer. The top anchor of all three extensometers was positioned about 4.6 m below the mine roof.

3.2. Host rock instruments

Model A-6 borehole extensometers [23] with fiberglass measurement rods and hydraulic anchors were installed in all but one of the pillars in the backfilled section to measure horizontal strain, identify when the skin of pillars began to spall, and compare strain on the backfilled side of the pillar to the strain on the side that was not backfilled. The extensometers were installed in B-size diamond drill holes with a shallow, large-diameter hole, counterbored at the collar to recess the anchor and protect the transducers from equipment and fly rock.

Four multiple-point, model A-6, vertical borehole extensometers were installed in the mine roof to measure roof sag and strata separation. Earth pressure cells and embedment strain gauges were placed in the backfill near these extensometers to verify roof sag and to measure the load applied to the backfill by the mine roof. Borehole extensometers were installed in the exterior side of the perimeter pillars at inclinations from 45° to 69° up from horizontal with the borehole collar approximately 3 m from the floor. Vertical extensometers were installed in the trapped pillars from a sublevel access drift about 6 m beneath the test area.

To monitor and evaluate stress changes in the host rock, model 4350 biaxial stressmeters [23] were installed at the mid-height of trapped pillars 102 and 103, the north abutment, and the west and

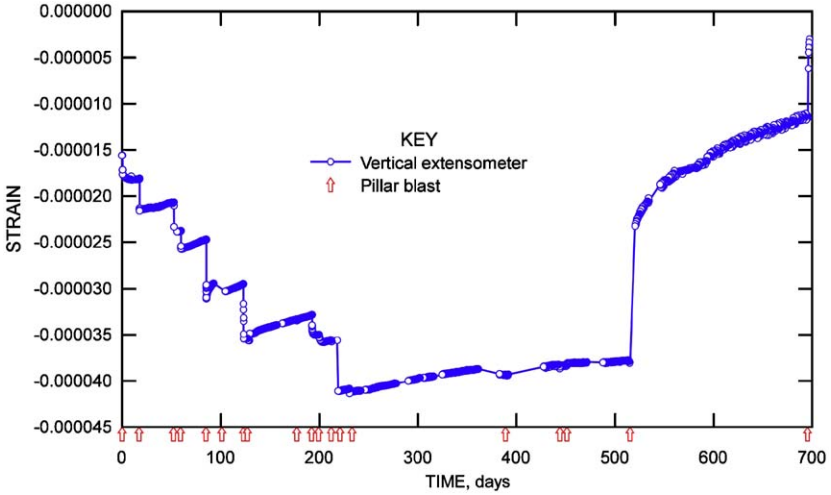

Fig. 12. Strain versus time during mining for extensometer in mine roof centered on pillars 95, 96, 104, and 105.

south barrier pillars. A description of this instrument and an explanation of its installation procedures and use in other mining applications is provided in [27].

4. Instrument results

For this study, compressive loading recorded by backfill instruments, and tensile displacements measured by extensometers in the mine roof and pillars are reported as positive. After nearly 16 years, 68% of the transducers installed in the backfilled area are still providing data. This percentage does not include instruments installed in pillars that were mined or biaxial stressmeters installed in the abutments and barrier pillars. Functioning instruments are shown in Fig. 6B. The location, orientation, and anchor lengths for working extensometers are listed in Table 2. Cables for the biaxial stressmeters installed in the north and south abutments were cut by mining equipment shortly after the instruments were installed and safe access could not be provided to repair the cables. Time in service for instruments that quit working are listed in Table 3. The biaxial stressmeters installed in the west abutment still provide data, but the stress changes obtained from these instruments became inexplicably high during mining of the trapped pillars. An analysis of the biaxial stressmeter data is not included in this paper. The earth pressure cell and embedment strain gauge centered mid-height in the backfill on pillars 92, 93, 101, and 102 and pillars 94, 95, 103, and 104 were previously reported as nonfunctional after five years because of the negative stresses and displacements that were recorded [19]; but this effect has since been attributed to decreasing temperature in the backfill. Transducer survivability is 90% for instruments installed mid-height in the backfill as opposed to 28% for those located in or near the mine roof. All but one of the instruments with cables strung in the backfill near the mine roof quit providing data when pillar 102 was mined, which suggests that the blast likely damaged their cables. The angled extensometer in pillar 113A was installed on the south side of the pillar with the transducers located at the borehole collar. A sealed cap was not used to protect the transducers from humid mine air, and consequently, one of them possibly failed because of corrosion.

Changes in instrument readings caused by blasts were identified by examining the data in Excel spreadsheets. A stress or strain reading that deviated from the trend on the day of the blast was considered to be caused by a blast. The selection was verified visually on plots of stress or strain versus time.

4.1. Backfill stress

Earth pressure cell measurements versus time are plotted in Figs. 8 and 9. For approximately the first 200 days, the general trend for the measurements is an immediate stress increase measured within 10 h after each blast, followed by a temperature-dependent stress decrease that can be attributed to cooling of the backfill mass. After day 200, the temperature effect is less prominent between blasts, and some of the instruments recorded time-dependent loading and abrupt changes not directly associated with the blasts. A possible reason for the abrupt changes, such as negative stress change, is uneven redistribution of stress as the mine roof settled on the backfill. After day 500, the slope of the lines are generally positive, indicating that the effect of temperature is small compared to time-dependent loading. This is

Table 2
Location, orientation, and anchor lengths of extensometers functioning after 16 years.

Instrument	Location	Dip[a] (deg)	Distance from collar or base (m)	
			Anchor 1	Anchor 2
VFX[b]	Northwest of pillar 103	90	11.89	
BX[c]	Pillar 113A	0	4.39	7.24
BX	Pillar 113A	52	5.79	10.97
BX	Centered in mine roof on 95, 96, 104, 105	90	10.87	

[a] Dip Angle up from the horizontal (positive).
[b] Vertical backfill extensometer.
[c] Borehole extensometer.

Table 3
Time in service for instruments currently not working.

Instrument	Location	Time in service (yrs)	Comments
VFX[a]	N of 104	0.39	
VFX	SE of 93	1.24	Damaged when pillar 102 mined
EPC[b]	Centered near top of backfill on 103, 104, 112, 113	1.24	Damaged when pillar 102 mined
EPC	Centered near top of backfill on 104, 105, 113, 114	1.24	Damaged when pillar 102 mined
VFX	Centered in mine roof on 93, 94, 102, 103	1.24	Damaged when pillar 102 mined
VBX[c]	Centered in mine roof on 102, 103, 111, 112	1.24	Damaged when pillar 102 mined
VBX	Centered in mine roof on 104, 105, 113, 114	1.24	Damaged when pillar 102 mined
ESG[d]	Centered near top of backfill on 93, 94, 102, 103	1.29	Damaged shortly after pillar 102 mined
ESG	Centered mid-height in backfill on 92, 93, 101, 102	6.68	
ESG	Centered mid-height in backfill on 94, 95, 103, 104	8.18	
ABX[e]	Pillar 113A, short anchor	11.82	Transducer located on exposed side of pillar

[a] Vertical backfill extensometer.
[b] Earth pressure cell.
[c] Vertical borehole extensometer.
[d] Embedment strain gauge.
[e] Angled borehole extensometer.

Table 4
Stress changes measured during and after pillar extraction.

Earth pressure cell location	Calculated initial stress (kPa)	Sum of changes measured within 10 h after each pillar extraction (kPa)	Sum of changes measured between each pillar extraction (kPa)	Change from installation to end of mining (kPa)	Post-mining change (kPa)	Change from installation to last reading (kPa)
93M[a]	190	379	12	581	1229	1810
94M	190	600	195	985	643	1628
95M	190	758	−122	826	208	1034
96T[b]	63	296	157	516	243	759
96M	190	1082	111	1383	1043	2426
101M	190	152	146	488	208	696
102M	190	1096	257	1543	126	1669
103M	190	938	69	1197	339	1536
104M	190	37	141	368	498	866
105M	190	655	158	1003	312	1515
Average	NA	599	112	889	485	1374
Standard deviation	NA	377	106	403	377	547

[a] Centered midheight in backfill on pillars 92, 93, 101, 102.
[b] Centered near top of backfill on pillars 95, 96, 104, 105.

consistent with temperature data collected in CRF that was about 23 m wide, 5 m high, and 31 m long. In general, temperature change in this rockfill sill was negligible after about 400 days [25].

Stress changes measured by the earth pressure cells during various time periods are compared in Table 4. The total stress increase for the earth pressure cells, from the time of their installation to the end of mining of the backfilled area, ranges from 370 kPa to 1.5 MPa, with an average equal to 900 kPa. The standard deviation for the total stress changes during this period is 400 kPa, indicating that the stress distribution on the backfill was not uniform. The average total stress increase that was measured between blasts is 19% of the average total stress increase recorded immediately after each pillar blast. The 30-day UCS for 15-cm-diam samples cored from backfilled stopes with similar constituents is 5.65 MPa, and the 28-day UCS for laboratory-prepared specimens of this backfill mix is 8.3 MPa [28], indicating that the backfill remained in the elastic range. Visual observations confirm instrument data that the backfill remained in a stable condition during mining, as illustrated in Fig. 13.

The stress measured by the earth pressure cells after the pillars in the backfilled area were mined, or "post-mining" period, are plotted versus time in Figs. 14 and 15. Regression lines for these data are described by

$$\sigma(t) = A \ln(t) - B, \quad (1)$$

where σ is compressive stress in kPa, t is time in days, and A and B are parameters calculated from regression analyses. R-squared values for these plots range from 0.79 to 0.98. Stresses recorded on day 1917 for two earth pressure cells, which are plotted between the dashed lines on the graphs, appear to be erroneous and are not included in the regression data set. Mining the eight pillars between the south barrier pillar between days 1974 and 2181 had no apparent effect on the long-term trend of the stress-versus-time data.

The average post-mining stress change is 35% of the total stress change. This figure may be slightly high because some of the time-dependent loading between blasts was likely masked by temperature-induced stress decrease. For two of the earth pressure cells, post-mining stress change is greater than the total stress change during mining. This emphasizes the importance of incorporating time-dependent loading into long-term stability design as well as incorporating a factor of safety for nonuniform loading.

The maximum stress change from the time the instruments were installed to the last reading that was taken, approximately 16 years later, is 2.4 MPa. This value is 42% of the average UCS of specimens prepared from core samples of a placed backfill with similar constituents [28], indicating that the backfill remained stable. Periodic visual observations confirm this conclusion.

Fig. 13. Stable backfill after pillar extraction.

4.2. Backfill strain

As shown in Figs. 10 and 11, the general trend for the embedment strain gauges and the vertical fill extensometer during pillar mining was similar to that of the earth pressure cells. The instruments responded to each pillar blast with compressive strain, followed by temperature-induced tensional strain. Strain measured by the embedment strain gauge centered mid-height on pillars 104, 105, 113, and 114 follows the same trend as the other embedment strain gauges, but is significantly larger in magnitude. The earth pressure cell located near this instrument is in the same range as the other earth pressure cells, indicating that the large embedment strain gauge readings were caused by some mechanism limited to a small volume of backfill around the instrument, but the mechanism is unknown. There also appears to be a local effect on the embedment strain gauge located mid-height to pillars 95, 96, 104, and 105 exhibited by apparent tensile strain. A possible cause for this apparent tension is aggregate that bridged over the embedment strain gauge and shielded the

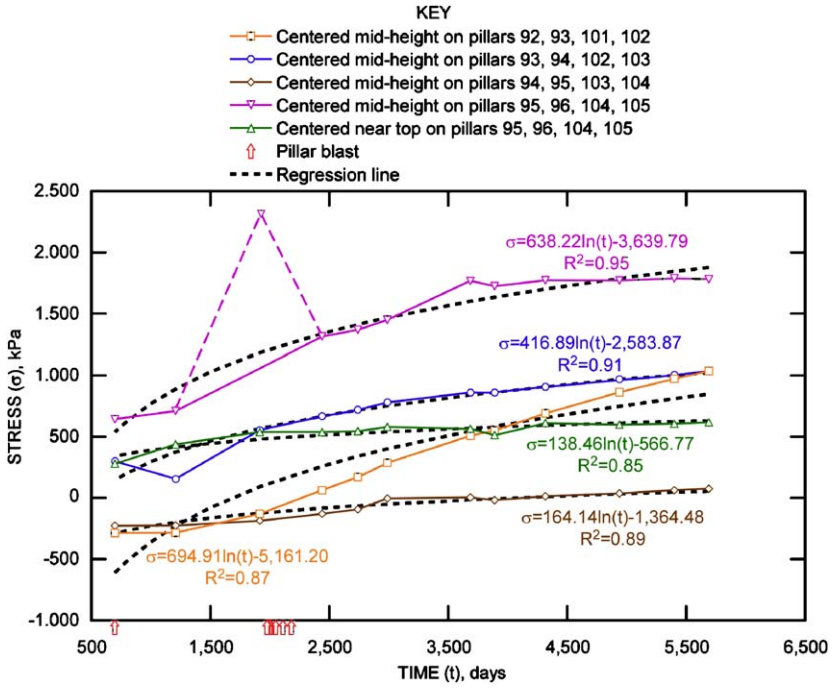

Fig. 14. Post-mining stress versus time for earth pressure cells in north drift.

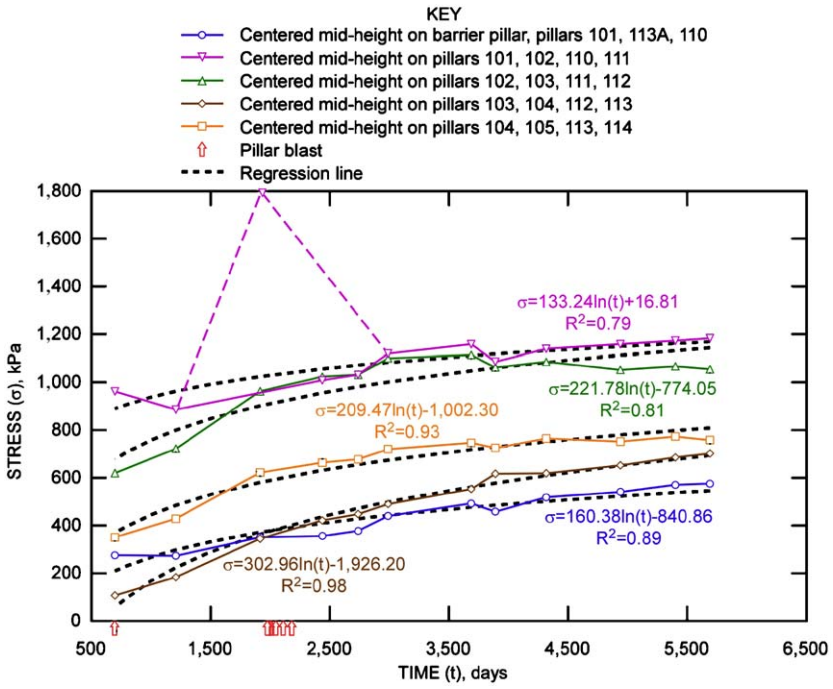

Fig. 15. Post-mining stress versus time for earth pressure cells in south drift.

instrument from loading, combined with the effect of backfill cooling.

Table 5 compares strain changes measured by the embedment strain gauges during various time periods. The total strain increase recorded by the embedment strain gauges, from the time that they were installed to the time when the last pillar in the backfilled section was mined, ranges from 140 to 3514 με, with an average equal to 746 με and standard deviation equal to 1,135 με. Hooke's Law was used to calculate initial strain. For this calculation, initial stress was obtained by multiplying the specific weight of the backfill by the depth of the backfill over the instrument, and the deformation modulus was calculated from earth pressure cell and embedment strain gauge readings that were recorded during mining. The average total strain increase that was measured between blasts is 42% of the average total strain increase recorded within 10 h after each pillar blast.

A natural log function describes post-mining strain-versus-time data, as shown in Figs. 16 and 17, with *r*-squared values ranging from 0.30 to 0.99. The average post-mining strain in the backfill is 28% of the total measured strain. Knowledge of this general trend in time-dependent behavior could be useful for assessing the long-term stability of other backfilled areas.

Table 5
Microstrain changes measured during and after pillar extraction.

Embedment strain gauge location	Calculated initial strain (με)	Sum of changes measured within 10 h after each pillar extraction (με)	Sum of changes measured between each pillar extraction (με)	Change from installation to end of mining (με)	Post - mining change (με)	Change from installation to last reading (με)
94[a]	101	1	38	140	31	171
96	101	111	100	312	−55	257
101	101	0	60	161	282	443
102	101	60	42	203	92	295
103	101	422	43	566	598	1164
104	101	155	132	388	323	711
105	101	2325	1088	3514	983	4497
103VFX[b]	69	581	33	683	28	711
Average	NA	457	192	746	285	1031
Standard deviation	NA	783	364	1135	353	1437

[a] Centered midheight in backfill on pillars 93, 94, 102, 103.
[b] Vertical fill extensometer northwest of pillar 103.

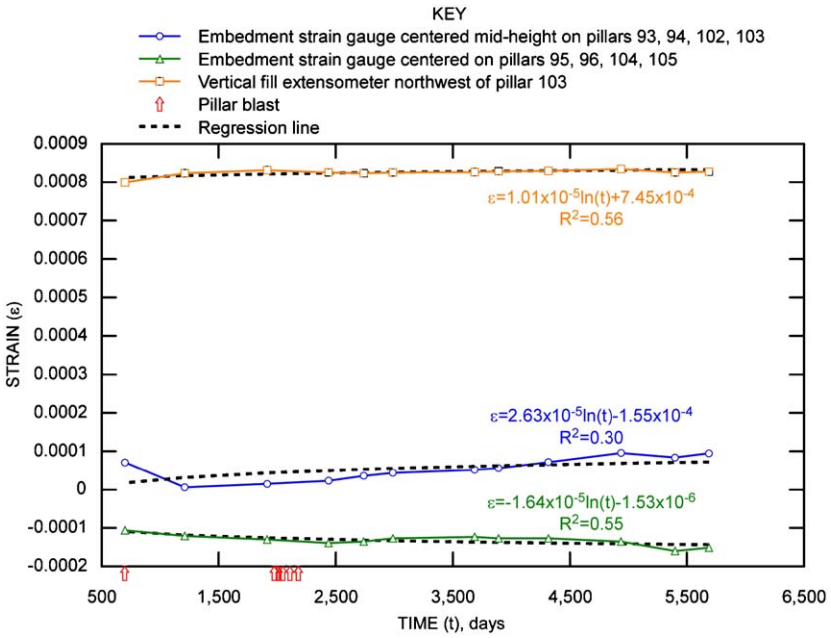

Fig. 16. Post-mining strain versus time for embedment strain gauges and vertical fill extensometer in north drift.

4.3. Pillar and roof strain

Measurements from the horizontal two-point borehole extensometer in pillar 113A demonstrate the effect of confinement provided by backfill on long-term pillar dilation. Backfill is placed on the north side of the pillar and the south side is unconfined. As shown in Fig. 18, the extensometer recorded a higher strain rate on the confined side of the pillar until day 515 when pillar 104 was mined. A possible cause for this high initial strain rate, despite confinement by the backfill, is the highly fractured condition of the north side of the pillar's skin that was observed during the installation of the extensometer. The trend reversed on day 515, and by day 1207 the horizontal strain rates on each side of the pillar were equal. By day 5689, the total measured strain on the unconfined side was over twice the strain on the confined side. Strain rate for the last 290 days, calculated by using the final two readings, was 0.17 με/day for the unconfined side and 0.025 με/day for the confined side; therefore, the strain rate for the unconfined side of the pillar is 6.8 than the rate for the confined side during the final 290 days of measurements.

Strain calculated from displacements recorded by the angled extensometer installed from the south side of pillar 113A is plotted against time in Fig. 19. The extensometer recorded compressive strain between the two deepest anchors during mining, indicating that the mine roof loaded the pillar. Strain, measured between the middle and collar anchors, did not substantially change during this time period. The general trend for both segments of the extensometer after mining, was increasing tension at approximately the same rate, indicating that the pillar was dilating. Another extensometer, installed from the north side of the pillar at the same angle as the one installed from the south side, would be necessary to compare the effect of confinement by the backfill.

Fig. 12 shows that the vertical borehole extensometer in the mine roof that is centered on pillars 95, 96, 104, and 105 measured compressive strain after each pillar was mined, followed by time-dependent tensional strain, up to day 233. A large component of the time-dependent strain is likely temperature-induced because the backfill mass was cooling. Pillar blasts had little effect on measured strain after day 233, until day 515 when support for the

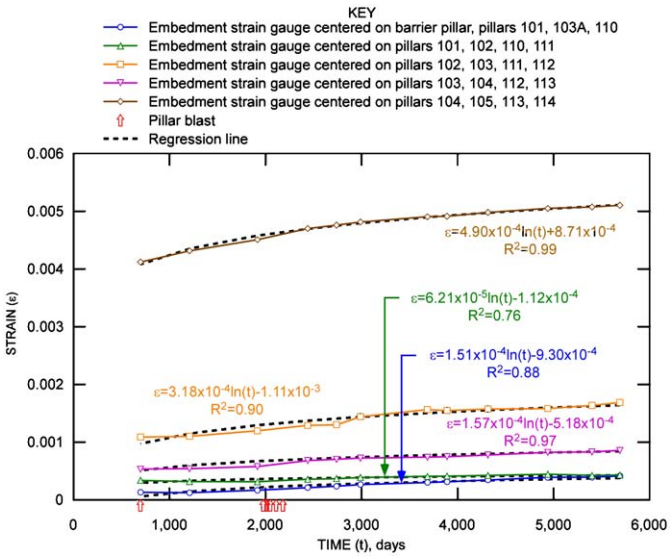

Fig. 17. Post-mining strain versus time for embedment strain gauges located mid-height to pillars in south drift.

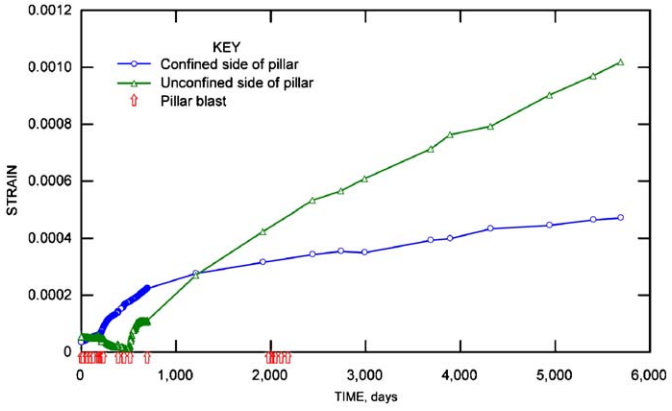

Fig. 18. Horizontal strain versus time for extensometer in pillar 113A.

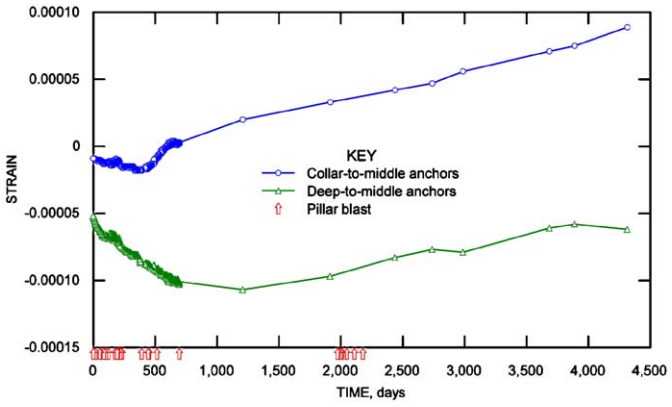

Fig. 19. Strain versus time for angled extensometer in pillar 113A.

mine roof near the vertical extensometer was reduced by mining pillar 104. The extensometer responded with tensional strain, followed by time-dependent tensional strain. A similar pattern was recorded in response to the extraction of pillar 103 on day 695. Post-mining measurements plotted in Fig. 20 indicate that the instrument measured tensional strain until day 1914, after

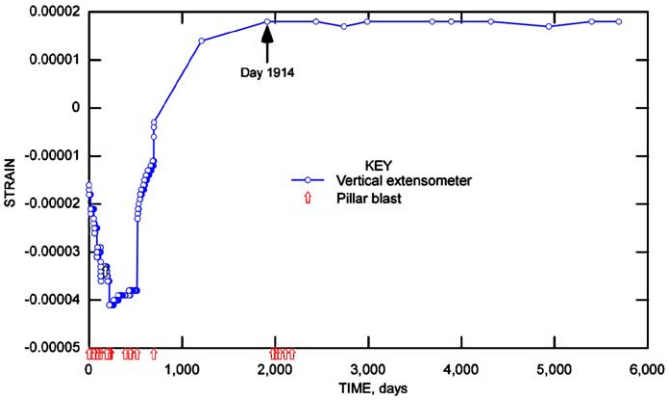

Fig. 20. Strain versus time for extensometer in mine roof centered on pillars 95, 96, 104, and 105.

which strain change was insignificant. This further confirms that temperature-induced tension had ceased.

5. Numerical modeling

A three-dimensional, finite-element program, UTAH3 [29], was used to model the excavation and backfill sequence [13]. A continuum model was chosen because Area 5 did not contain major faults that could dominate material behavior. The modulus of deformation was reduced from its laboratory value to account for the joint sets. The yield criterion in UTAH3 is Drucker–Prager, in which strength is dependent on all three principal stresses, and the associate flow rules are applied for determining strains in yielded elements. Elastic perfectly plastic material behavior was used for the rock mass because of the confinement provided by the backfill. This material property was also chosen for the backfill because it was assumed that the large volume of material would provide self confinement; also, laboratory triaxial tests on rockfill specimens, similar in composition to the backfill in Area 5, indicate that the stress-versus-strain relationship can be idealized with an elastic perfectly plastic material model [30].

The finite-element mesh contained 252,000 elements representing a rock mass 271 x 271 x 535 m with a 18.3-m-thick mining horizon 366 m below the surface and 151 m above the bottom of the rock mass block. Fig. 3 shows the model's boundary in plan view. Rollered boundary conditions were used on all sides of the block except the top, which was free to move vertically. Cubes 4.6 m on a side simulated the rock mass from 9 m below to 46 m above the mining horizon. The remaining elements were 4.6 x 4.6 x 9.1 m with the longest dimension along the vertical axis. The entire mesh is shown in Figs. 21 and 22 depicts a discretized section containing a room and two pillars. Vertical coordinates of the nodes in the finite element mesh were adjusted to coincide with the boundaries between rock types from a generalized stratigraphic column of Area 5. The idealized excavation shape was realistically represented by using these brick-shaped elements because pillar boundaries nearly coincided with the faces of the bricks. Node coordinates for pillars 93, 102, 103 and 104 were adjusted to conform to pillar boundaries more accurately. Each pillar blast or excavation step that was modeled required about 12 h to run on a Dell Precision 530 work station.

Laboratory material properties for the rock types used in the model are listed in Table 6. Properties for dolomite were obtained from unconfined uniaxial compression tests on specimens prepared from BX core recovered from the instrument holes. The specific weight of these specimens was averaged for input into the model. Dolomitic mudstone and shale property values

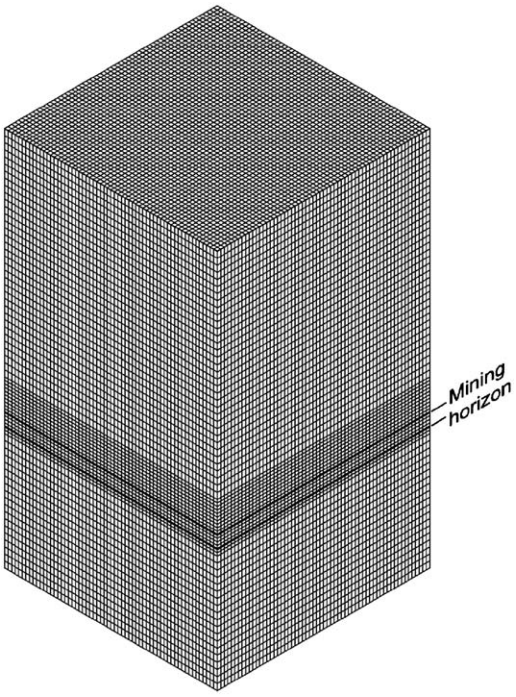

Fig. 21. Finite-element mesh.

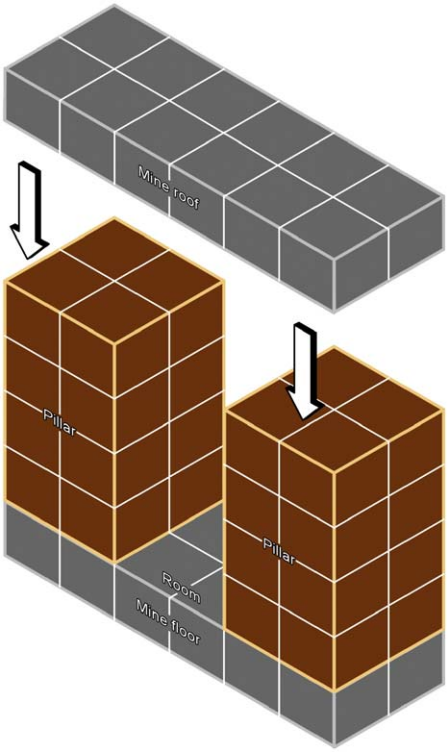

Fig. 22. Discretized room, pillars, mine roof, and mine floor.

were based on published laboratory tests [31]. The deformation modulus for the backfill was calculated using data recorded by pairs of earth pressure cells and embedment strain gauges placed at the same location in the backfill by dividing the sum of the stress changes measured immediately after a pillar blast by the sum of the corresponding strain changes. Strength values for the backfill were estimated from UCS tests conducted on laboratory-prepared specimens and core samples extracted from a backfilled stope with constituents similar to the Buick Mine backfill [28].

In situ stresses that were used as the initial stress state in the numeric model are listed in Table 7. The were obtained by overcoring four hollow inclusion stress cells (developed by Australia's Commonwealth Scientific and Industrial Research Organization) in the north part of the Buick Mine. Measurements were taken at borehole depths between 13.4 and 16.5 m in an abutment of a room-and-pillar section approximately 72 m wide and 305 m long. Cube-shaped pillars in this area measured 7.6 m on each side and rooms were 10.7 m wide [32].

UTAH3 [29] was calibrated using blast-induced displacement readings recorded by the vertical borehole extensometers in the trapped pillars [13]. Model-predicted strains were plotted against strains calculated from measured displacements and a line was fit to the data using regression analysis. The initial modulus of deformation for dolomite, equal to 37.2 GPa, used in the model was based on results of previous calibrations using a three-dimensional, boundary-element program and a two-dimensional finite-element program [18]. This value is approximately 45% of the laboratory deformation modulus. Deformation modulus values for dolomitic mudstone and shale were also reduced by 45%.

The slope of regression line for calculated versus measured strain was equal to 0.85, indicating that the initial modulus could have been further reduced by multiplying it by 0.85 to achieve a slope equal to one for the regression line. However, this would reduce the difference between calculated and measured strain for only a few pair of points with large strain and increase the difference for the majority of pairs. For this reason, the initial modulus was not reduced.

The UCS of dolomite was reduced by comparing model-calculated changes in vertical strain in trapped pillar 103 to measured strain. On day 192 when pillars 112 and 4 were blasted, measured strain was nine times that of elastic calculated strain, indicating that pillar 103 failed. Iterative computer runs were made with decreasing UCS values for dolomite until the model produced failed elements in pillar 103 when pillars 112 and 4 were mined. This value is 43 MPa or about 40% of the laboratory UCS value of dolomite. Tensile strength was also reduced by 40%.

Reduced deformation modulus and unconfined strength values obtained by calibrating UTAH3 compare favorably to those calculated using empirical methods. A rock mass modulus equal to 44 GPa, or 52% of the average laboratory deformation modulus, was calculated using the following empirical relationship [33].

$$E_M = 2 \times RMR - 100, \tag{2}$$

where E_M is the rock mass deformation modulus in GPa.

The Hoek–Brown generalized failure criterion for jointed rock [34] was used to estimate the UCS of the rock mass. This formula is

$$\sigma_1' = \sigma_3' + \sigma_{ci}(m_b\sigma_3'/\sigma_{ci} + s)^a, \tag{3}$$

where σ_1' and σ_3' are the maximum and minimum effective stresses at failure, m_b is the value of the Hoek–Brown constant for the rock mass, s and a are the parameters that depend upon rock mass characteristics, and σ_{ci} is the UCS of the intact rock. For an estimate of the UCS of the rock mass, Eq. (3) reduces to

$$\sigma' = \sigma_{ci}s^a, \tag{4}$$

where

$$s = \exp[(GSI - 100)/9], \tag{5}$$

where GSI is the geological strength index developed in [35,36] to estimate the reduction in rock mass strength for different geological conditions; it is presented in tabular form in [37].

Table 6
Average laboratory rock properties and in situ backfill properties.

	Young's modulus (MPa)	Unconfined compressive strength (MPa)	Tensile strength (MPa)	Specific weight (kg/m^3)	Poisson's ratio
Dolomite	84,800	108.9	10.9	2563	0.26
Dolomitic mudstone	34,500	54.0	5.4	2563	0.25
Shale	17,200	54.0	5.4	2195	0.25
Cemented backfill	1910	6.9	0.7	2114	0.30

Table 7
Major principle stresses from hollow inclusion stress cells.

Stress (MPa)	Azimuth (deg)[a]	Dip (deg)[b]
24.52	240	1.6
7.98	128	85.8
3.44	149	−3.9

[a] Angle clockwise from north is positive.
[b] Angle down from horizontal is positive.

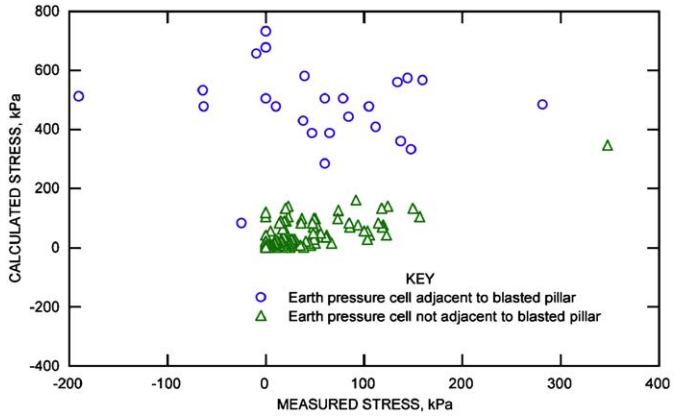

Fig. 23. Calculated versus measured stress in backfill.

Based on the existence of two joint sets and one set of bedding planes in Area 5, the GSI value is about 80. For a GSI value greater than 25, the parameter a is equal to 0.5. Using Eqs. (4) and (5), the reduction factor (s^a) in UCS for a GSA value of 80 is 0.33.

The initial modulus of deformation of the backfill was not adjusted because it was calculated from in situ measurements. There is scatter in the measured versus model-calculated stress changes as shown in Fig. 23, however, these data help explain the interaction of the backfill and mine roof. The plot contains a cluster of points in which the calculated stresses are significantly larger than measured stress changes and five points representing negative measured stress changes. Inspection of the data containing the large difference between measured and calculated stress changes reveals that these points were recorded when at least one of the four pillars surrounding the earth pressure cell was mined. With loss of local support provided by nearby pillar or pillars, the roof likely settled on the uneven backfill surface, filling voids left by the belt slinger, but not significantly loading the backfill. In the numerical model, the backfill was in complete contact with the mine roof, enabling the backfill to react immediately to vertical sag in the roof and produce higher calculated stresses than those that were measured. Other possible reasons for the discrepancy in stress magnitude are varying material properties in the backfill and mine roof, and mine geometry that is not accounted for in the idealized model.

The negative changes recorded by the earth pressure cells may have been caused by point contacts between the mine roof and backfill, yielding and redistributing stresses. Based on this interpretation of the interaction of the backfill and mine roof, the magnitude of measured stress changes are realistic.

6. Conclusions

This case study in a backfilled section of a lead/zinc/copper room and pillar mine suggests the following conclusions:

Post-mining stress and strain measured in the backfill are significant compared to total measured stress and strain. The average stress change measured in the backfill after mining is 35% of the total average stress change. The average post-mining strain in the backfill is 28% of the total strain that was measured. Accounting for this time-dependent loading into the design of backfilled sections could improve the assessment of long-term stability. In this study, the strength of the backfill was adequate to carry this additional load, and remained stable for 16 years.

Backfill limits pillar dilation. The total measured strain on the unconfined side of a support pillar was over twice the strain on the side confined by backfill. The strain rate for the unconfined side of the pillar was 6.8 times larger than the rate for the confined side for the last 290 days that were measured.

Vibrating wire instruments provide reliable long-term data provided that the instruments and their cables are adequately protected. After nearly 16 years, 68% of the transducers that were installed in the Area 5 backfilled test area, and not mined out, still provide data. Based on long-term laboratory tests on vibrating wire transducers performed by other researchers, these data are a true function of material behavior because vibrating wire transducers have repeatable readings and insignificant drift.

A natural logarithm function in the form $\sigma(t) = A\ln(t) - B$ describes post-mining stress measured by earth pressure cells and strain measured by embedment strain gauges, as a function of time. R-squared values for the earth pressure cell plots range from 0.79 to 0.98, and from 0.30 to 0.99 for the embedment strain gauge plots. Knowledge of this general trend in time-dependent behavior could be useful for assessing the long-term stability of other backfilled areas.

Numerous instruments placed throughout the backfill aided in interpreting the interaction of the backfill and host rock. Data from earth pressure cells in the backfill indicate that the backfill was not loaded uniformly by the mine roof. This was verified by plotting stress changes in the backfill (calculated by a three-dimensional, finite-element model of Area 5) versus measured stress changes in the backfill. Calculated stress was much larger than measured stress in some cases because the mine roof was not 100% in contact with the backfill.

Recording temperature of the backfill and host rock would facilitate data interpretation for backfill studies. For example, in this study, time-dependent stress increase between pillar blasts could not be measured because it was masked by decreasing temperature in the backfill. The time at which backfill cooling

ceased was interpreted from extensometer displacements in the mine roof.

Backfill can be used as primary long-term ground support and subsidence abatement in hard rock mines provided that the initial design strength of the backfill accounts for time-dependent loading. In this study, the strength of the backfill was adequate to carry time-dependent loading, and remained stable for 16 years.

Acknowledgments

The authors wish to express their appreciation to the following members of The Doe Run Co. who were instrumental in the success of the A-5 Study at the Buick Mine, Boss, Missouri: Bill Lane, Vice President of Mining & Technical Development, for initiating the research, assisting in the development and implementation of the geotechnical instrumentation plan, and supplying most of the instruments and data acquisition equipment; Bob Roscoe, Vice President of Mining and Milling Operations in Missouri and Greg Sutton, Mine Manager, for their support installing instruments and maintaining data acquisition systems during the initial years of this study. We also wish to thank the many Doe Run employees who have periodically collected manual readings from the instruments over the intervening years following completion of mining in Area 5, in particular, Lori Young, Mine Engineer, and former employee Lyndon Clark. We gratefully acknowledge the efforts of the following employees of the NIOSH Spokane Research Laboratory, Spokane, WA: Mike Jones for collecting manual readings; Bob McKibbin and Curtis Clark for installing instruments; and Bob McKibbin and Mike Jenkins for determining in situ stress. We also wish to thank Tony Simmonds, International Projects Manager, Geokon, Inc., Lebanon, NH, for providing data from long-term pressure transducer tests; and Bill Pariseau, Department of Mining Engineering, University of Utah, for technical suggestions regarding this research.

Disclaimer

The findings and conclusions in this paper have not been formally disseminated by the National Institute for Occupational Safety and Health, and should not be construed to represent any agency determination or policy.

References

[1] Potvin Y, Thomas E, Fourie A. Handbook on mine fill. Nedlands, Australia: Australian Centre for Geomechanics; 2005.
[2] Landriault D. Backfill in underground mining. In: Hustrulid WA, Bullock RL, editors. Underground mining methods: engineering fundamentals and international case studies. Littleton, Colo: Society for Mining Metallurgy & Exploration; 2001. p. 601–14.
[3] Williams TJ, Bayer DC, Bren MJ, Pakalnis RT, Marjerison JA, Langston RB. Underhand cut and fill mining as practiced in three deep hard rock mines in the United States. In: Proceedings of the CIM conference exhibition, Montreal, 2007, p. 1–11.
[4] DeSousa E, Mottahes P, Coode A, Sellers B. Ten years of continuous monitoring in a mining panel. Int J Rock Mech Min Sci 1997;34:3–4 Paper No. 060.
[5] McNay LM, Corson DR. Hydraulic sandfill in deep metal mines. Spokane, Wash: Bur Mines, Spokane Mining Research Center, US Bur Mines Information Circular 8663, 1975.
[6] Herget G, Munroe SR. Utilization of salt tailings backfill at Denison-Potash Company. In: Hassani FP, Scoble MJ, Yu TR, editors. Proceedings of the fourth international symposium on mining with backfill. Montreal, 1989. p. 335–42.
[7] Beddoes RJ, Roulston BV, Streisel J. Field monitoring of salt tailings used as backfill in cut-and-fill potash mining. In: Hassani FP, Scoble MJ, Yu TR, editors. Proceedings of the fourth international symposium on mining with backfill. Montreal, 1989. p. 343–8.
[8] Gürtunca RG, Leach AR, York G, Treloar ML. In situ performance of cemented backfill in a deep-level South African gold mine. In: Glen HW, editor. Minefill 93, Johannesburg, South Africa, 1993. p. 121–8.
[9] Zhurin SN. Pore pressure control during underground tailings disposal. In: Stone D, editor. Minefill 2001, Proceedings of the seventh international symposium mining with backfill. Littleton, CO: Society for Mining, Metallurgy & Exploration; 2001. p. 127–32.
[10] Donovan J, Dawson J, Bawden WF. David Bell Mine underhand cut and fill sill mat test. In: Proceedings of the ninth international symposium on mining with backfill. Montreal, Can Inst of Mining Metall Petrol, 2007, paper 2467.
[11] Maleki H, Chaturvedi L. Prediction of room closure and stability of panel 1 in the waste isolation pilot plant. Int J Rock Mech Min Sci 1997;34:3–4 Paper No. 186.
[12] Steed C, Pitman W, Roberts D. Pillar optimization for initial design and retreat recovery. In: Peng SS, Mark C, Khair AW, editors. Proceedings of the 22nd international conference ground control in mining. Morgantown, WV, 2003. p. 86–94.
[13] Tesarik DR, Seymour JB, Yanske TR. Post-failure behavior of two mine pillars confined with backfill. Int J Rock Mech Min Sci 2003;40(2):221–32.
[14] Roberts DP, Lane WL, Yanske TR. Pillar extraction at the Doe Run Company 1991–1998. In: Bloss M, editor. Proceedings of the sixth international symposium mining with backfill. Victoria, Australia, 1999. p. 227–33.
[15] Yanske TR, Clark LM, Carmack JE. CRF pillar construction at the Doe Run Company. In: Stone D, editor. Minefill 2001, Proceedings of the seventh international symposium on mining with backfill. Littleton, Colo: Society for Mining, Metallurgy & Exploration; 2001. p. 337–49.
[16] Young LR, McIntire HE, Yanske TR. CRF backfill at the Doe Run Company 1991–2006. In: Proceedings of the ninth international symposium mining on with backfill. Montreal, Can Ins of Mining Metall Petrol, 2007, paper 2520.
[17] Lane WL, Yanske TR, Roberts DP. Pillar extraction and rock mechanics at the Doe Run Company in Missouri 1991–1999. In: Amadei B, Kranz RL, Scott GA, Smeallie PH, editors. Proceedings of the 37th US rock mechanical symposium. Rotterdam: Balkema; 1999. p. 285–92.
[18] Tesarik DR, Seymour JB, Yanske TR, McKibbin RW. Stability analysis of a backfilled room-and-pillar mine. Spokane, Wash: Bur Mines, Spokane Research Center, US Bur Mines Reports of Investigation 9565, 1995.
[19] Tesarik D, Seymour B, Yanske T. Long-term stability of a backfilled room-and-pillar mine. In: Leung CF, Tan SA, Phoon KK, editors. Proceedings of the fifth international symposium field measurements in geomechanics. Rotterdam: Balkema; 1999. p. 431–43.
[20] Choquet P, Juneau F, DeBreuille PJ, Bessette J. Reliability, long-term stability and gage performance of vibrating wire sensors with reference to case histories. In: Leung CF, Tan SA, Phoon KK, editors. Proceedings of the fifth international symposium field measurements in geomechanics. Rotterdam: Balkema; 1999. p. 49–54.
[21] McRae JB, Simmonds T. Long-term stability of vibrating wire instrument: one manufacturer's perspective. In: Sorum G, editor. Proceedings of the third international symposium field measurements in geomechanics. Rotterdam: Balkema; 1991. p. 283–93.
[22] Dunnicliff J. Geotechnical instrumentation for monitoring field performance. New York: Wiley; 1988.
[23] Geokon, Inc. Geokon: the world leader in vibrating wire technology. 〈http://www.geokon.com〉. Date accessed: 30 April 2008.
[24] Daigle L, Zhao JQ. Assessing temperature effects on earth pressure cells. Ottawa: Nat Res Counc of Canada; 2003, Res Resp 131; 2003.
[25] Tesarik DR, Seymour JB, Williams TJ, Martin LA, Jones FM. Temperature corrections to earth pressure cells embedded in cemented backfill. Cincinnati: US Department of Health & Human Services, Public Health Service, Centers for Disease Control and Prevention, National Institute for Occupational Safety and Health, NIOSH Reports of Investigation 9665, 2006.
[26] Sellers B. Temperature effects on earth pressure and concrete stress cells: some theoretical considerations. Geotech Instrum News 2000;18:23–4.
[27] Seymour JB, Tesarik DR, McKibbin RW, Jones FM. Monitoring mining-induced stress changes with the biaxial stressmeter. In: Leung CF, Tan SA, Phoon KK, editors. Proceedings of the fifth international symposium field measurements in geomechanics. Rotterdam: Balkema; 1999. p. 55–60.
[28] Brechtel CE, Baz-Dresch J, Knowlson JS. Application of high-strength backfill at the Cannon Mine. In: Hassani F, Scoble M, Yu T, editors. Proceedings of the fourth international symposium mining with backfill. Rotterdam: Balkema; 1989. p. 105–17.
[29] Pariseau WG. Interpretation of rock mechanics data. Salt Lake City: University of Utah, Contract H0220077 for US Bur Mines OFR-47(2)-80, vol. 2, 1978.
[30] Sainsbury D, Yuejun C, Thompson B. Investigation of the geomechanical characteristics of stabilized rockfill. In: Stone D, editor. Minefill 2001, Proceedings of the seventh international symposium mining with backfill. Littleton, Colo: Society for Mining Metallurgy & Exploration; 2001. p. 105–15.
[31] Farmer IW. Engineering properties of rocks. London: Butler & Tanner; 1968.
[32] Tesarik DR, McKibbin RW. Instrumentation and modeling of the north 140 section of Magmont Mine, Bixby, MO. Spokane: Bur Mines, Spokane Research Center, US Bur Mines Reports of Investigation 9215, 1989.
[33] Bieniawski ZT. Rock mechanics in mining and tunneling. Rotterdam: Balkema; 1984. p. 79–80.
[34] Hustrulid WA, Bullock BL, editors. Underground mining methods. Littleton, Colo: Society for Mining Metallurgy & Exploration; 2001.
[35] Hoek E. Strength of rock and rock masses. Int Soc Rock Mech News J 1994;2(2):4–16.
[36] Hoek E, Kaiser PK, Bawden WL. Support of underground excavations in hard rock. Rotterdam: Balkema; 1995.
[37] Hoek E, Marinos P, Benissi M. Applicability of the geological strength index (GSI) classification for weak and sheared rock masses: the case of the Athens schist formation. Bull Eng Geol Environ 1998;57(2):151–60.